Supporting Information

An insight into molecular structures, theoretical calculation and catalytic activities of novel heterotri-nuclear [$Cu^{II}_2Ce^{III}$] and heterohexa-nuclear [$Cu^{II}_4Y^{III}_2$] bis(salomo)-based complexes

Zhuang-Zhuang Chen, Wen-Ze Zhang, Ting Zhang, Yang Zhang and Wen-Kui Dong*

School of Chemical and Biological Engineering, Lanzhou Jiaotong University, Lanzhou 730070

Corresponding authors.

*E-mail: dongwk@126.com. Fax: +86-931-4938703.

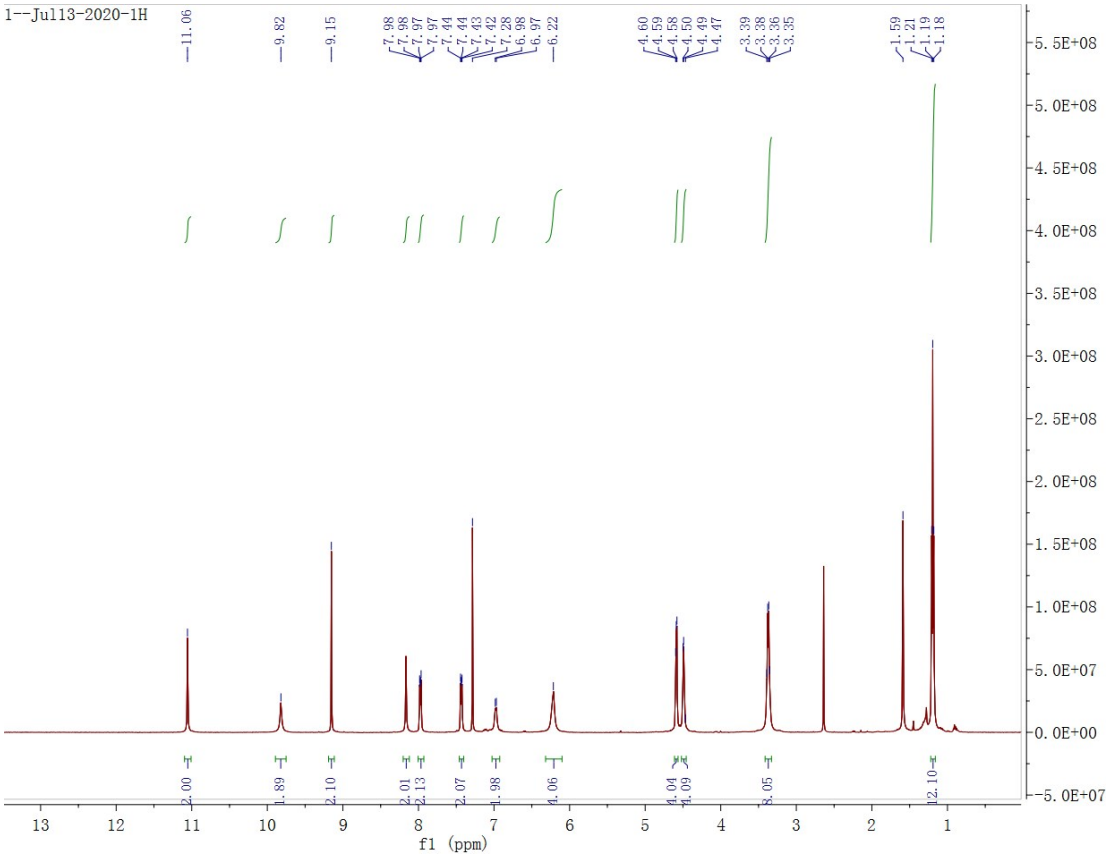

Figure S1 ^{1}H NMR spectrum of **1a** in $CDCl_3$.

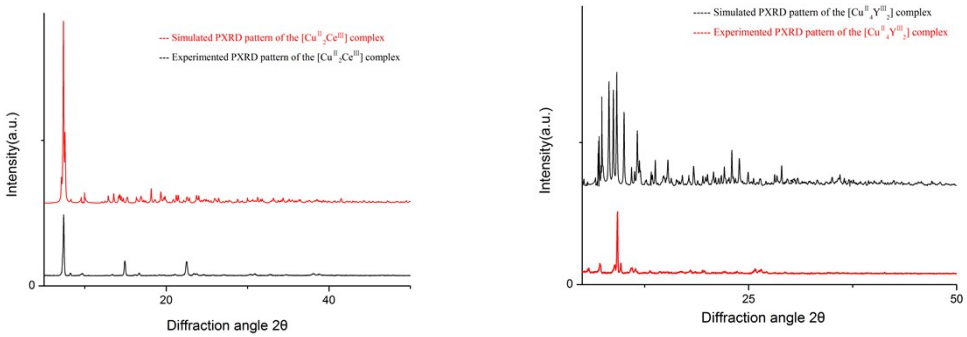

Fig. S2 Comparison of X-ray diffraction (PXRD) modes of simulated and experimental powders for the $[Cu^{II}_2Ce^{III}]$ complex and the $[Cu^{II}_4Y^{III}_2]$ complex.

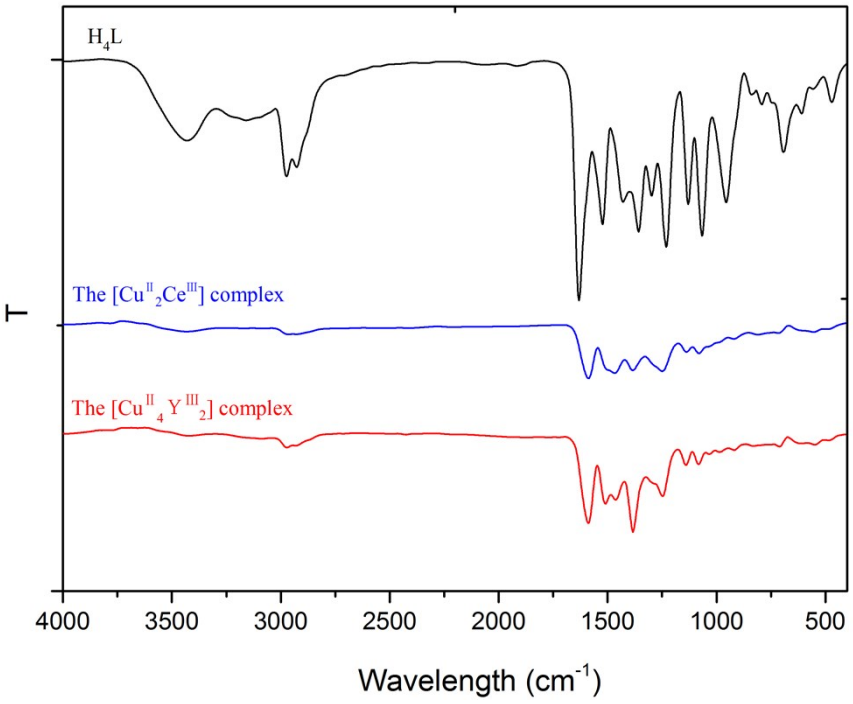

Fig. S3 FT-IR spectra of H_4L and its $[Cu^{II}_2Ce^{III}]$ and $[Cu^{II}_4Y^{III}_2]$ complexes.

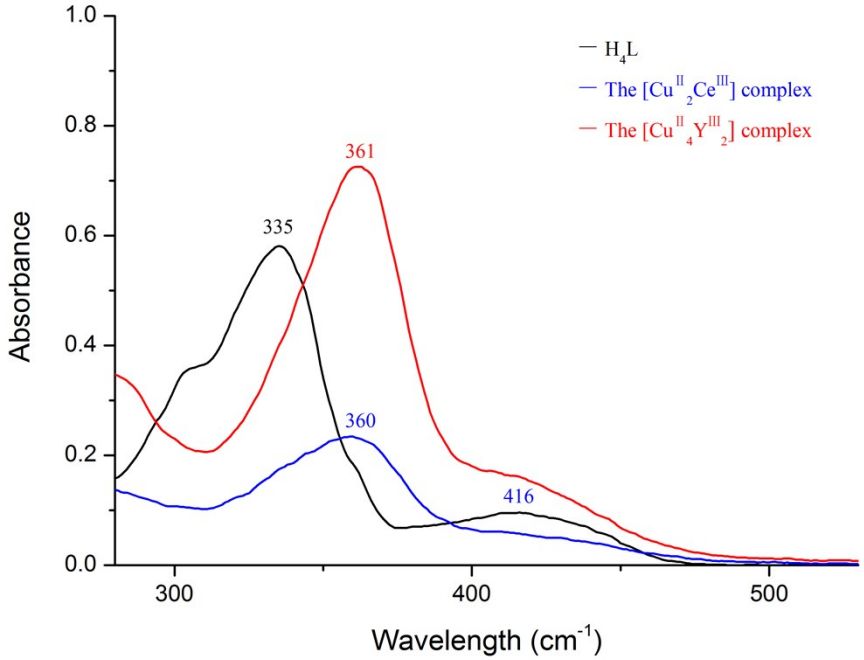

Fig.S4 UV–visible absorption spectra of H_4L and its corresponding $[Cu^{II}_2Ce^{III}]$ and $[Cu^{II}_4Y^{III}_2]$ complexes in DMF solution.

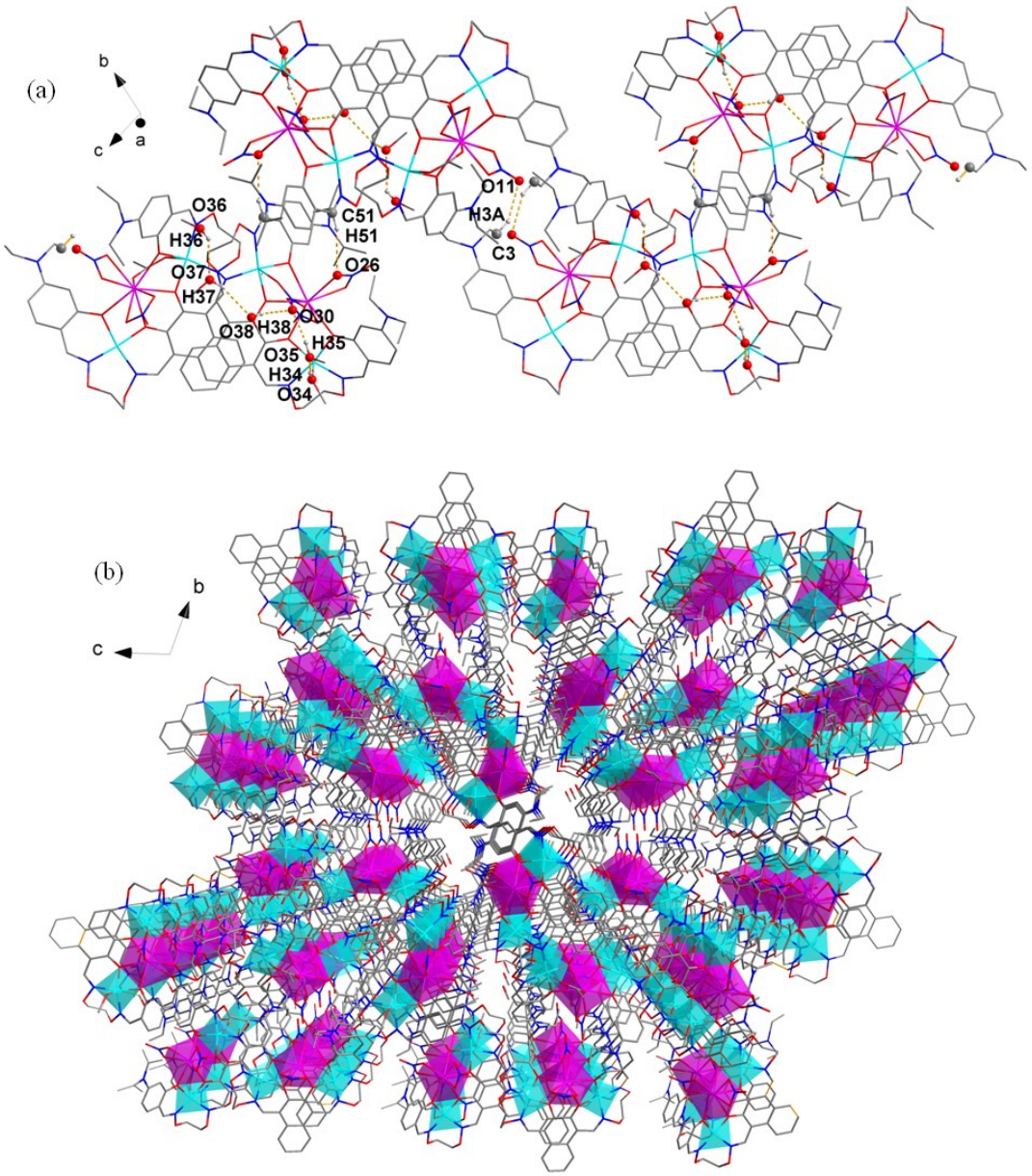

Fig. S5 (a) View of an infinite 2D supramolecular structure of the $[Cu^{II}_4Y^{III}_2]$ complex. (**b)** View of an infinite 3D supramolecular structure of the $[Cu^{II}_4Y^{III}_2]$ complex.

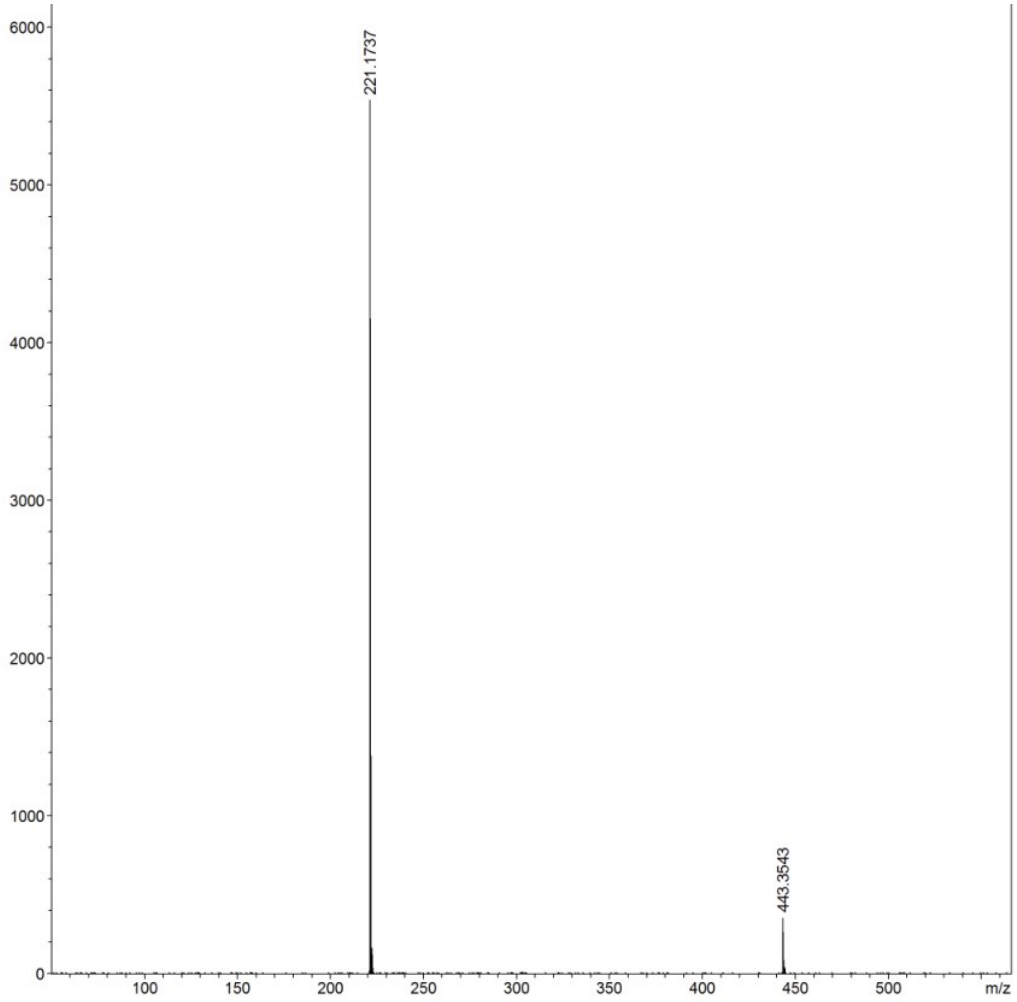

Figure. S6 Representative ESI-MS of 3,5-di-tert-butylquinone (3,5-DTBQ).

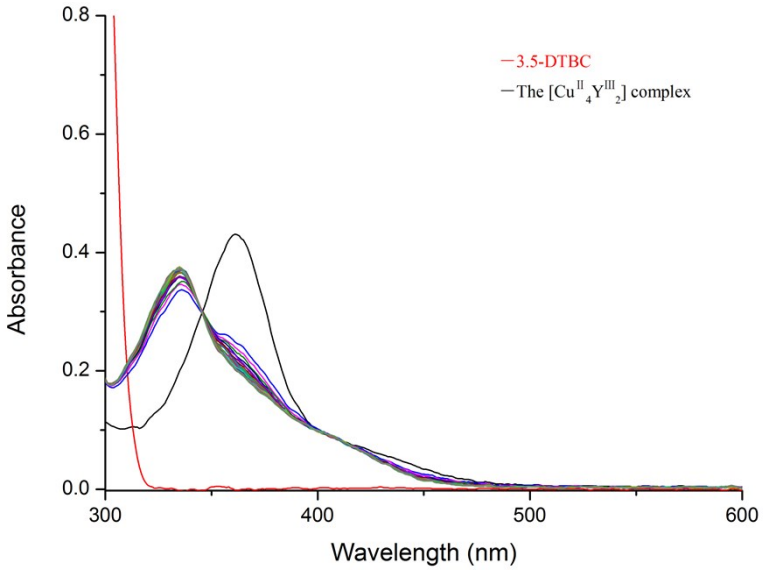

Fig. S7 Changes observedin UV-vis spectra of the [$Cu^{II}_4Y^{III}_2$] complex in MeCN/DMF upon addition of 300-fold 3,5-DTBC.

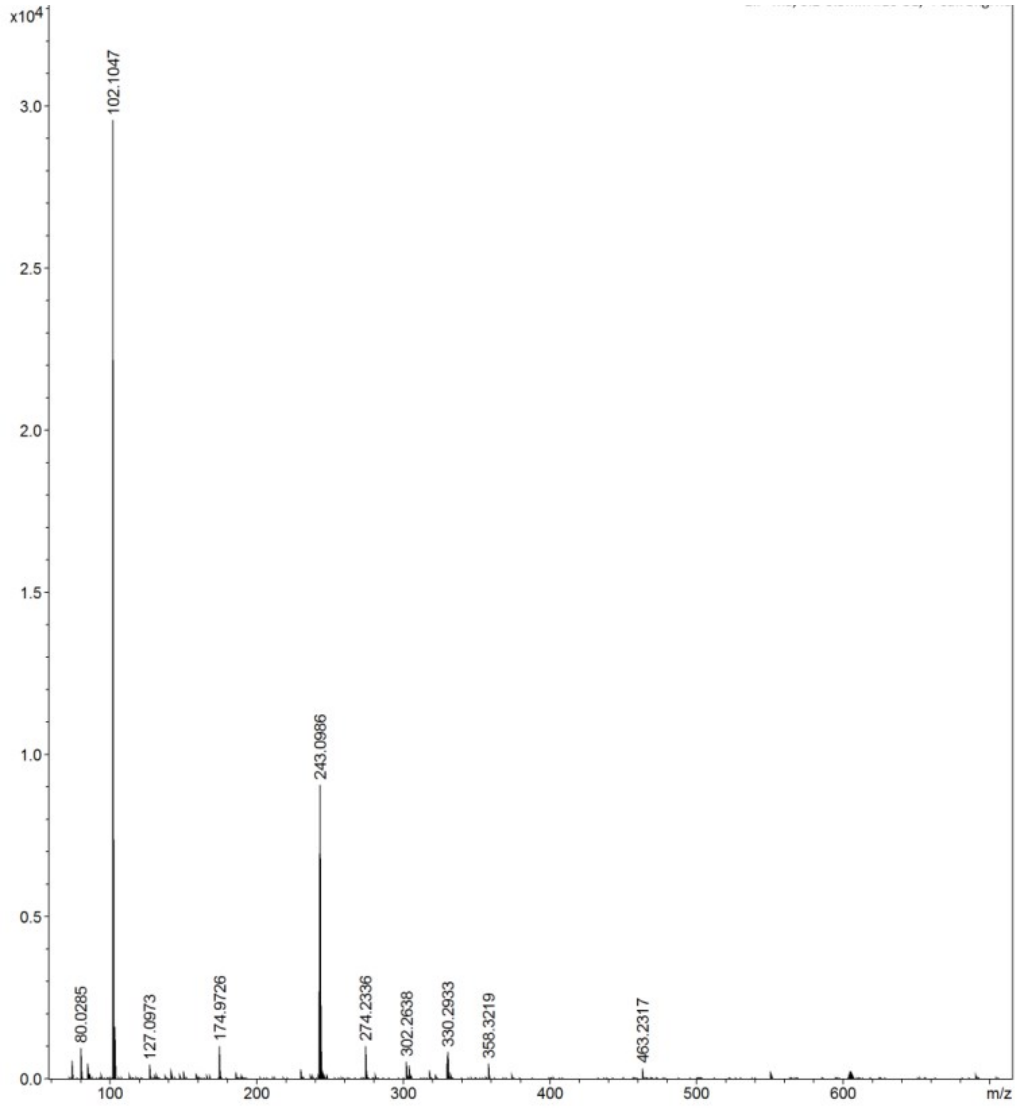

Fig. S8 The molecular ion peak of the intermediate in the catalytic oxidation process in MeCN/DMF solution

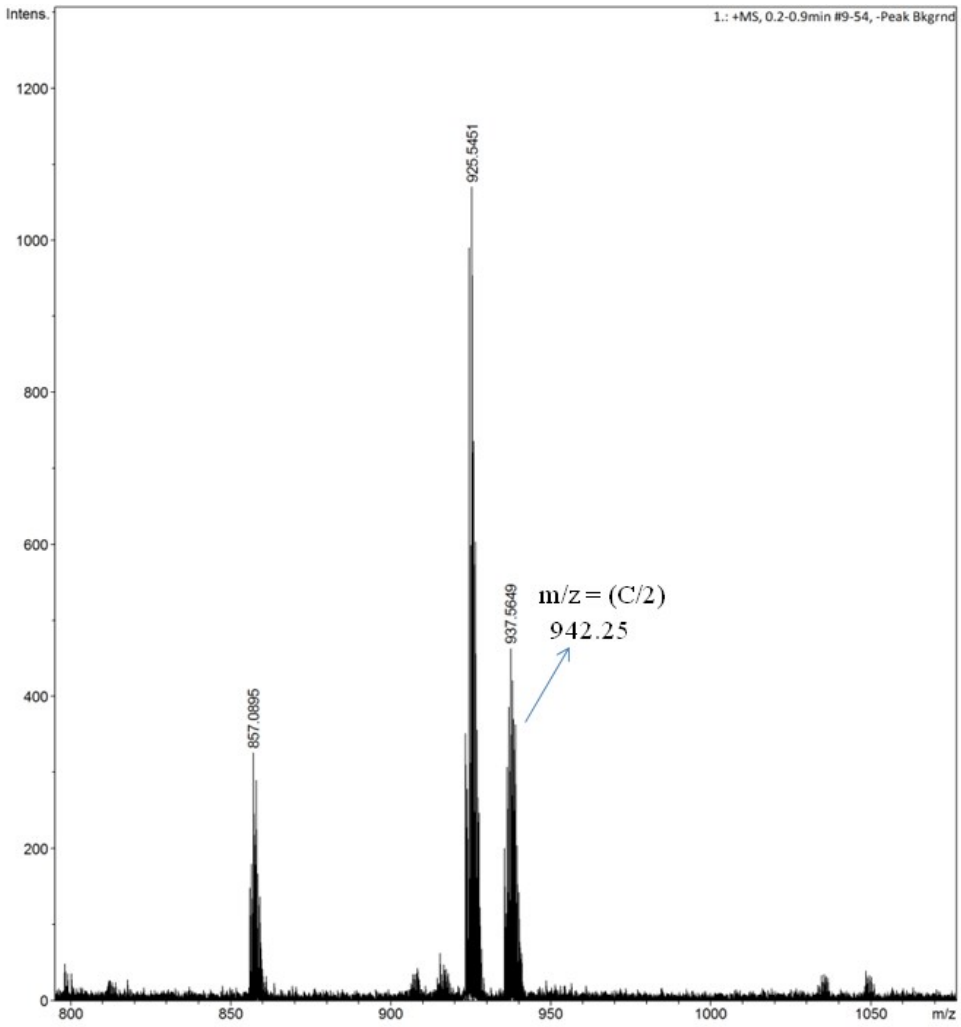

Fig. S9 The molecular ion peak of the intermediate in the catalytic oxidation process in MeCN/DMF solution

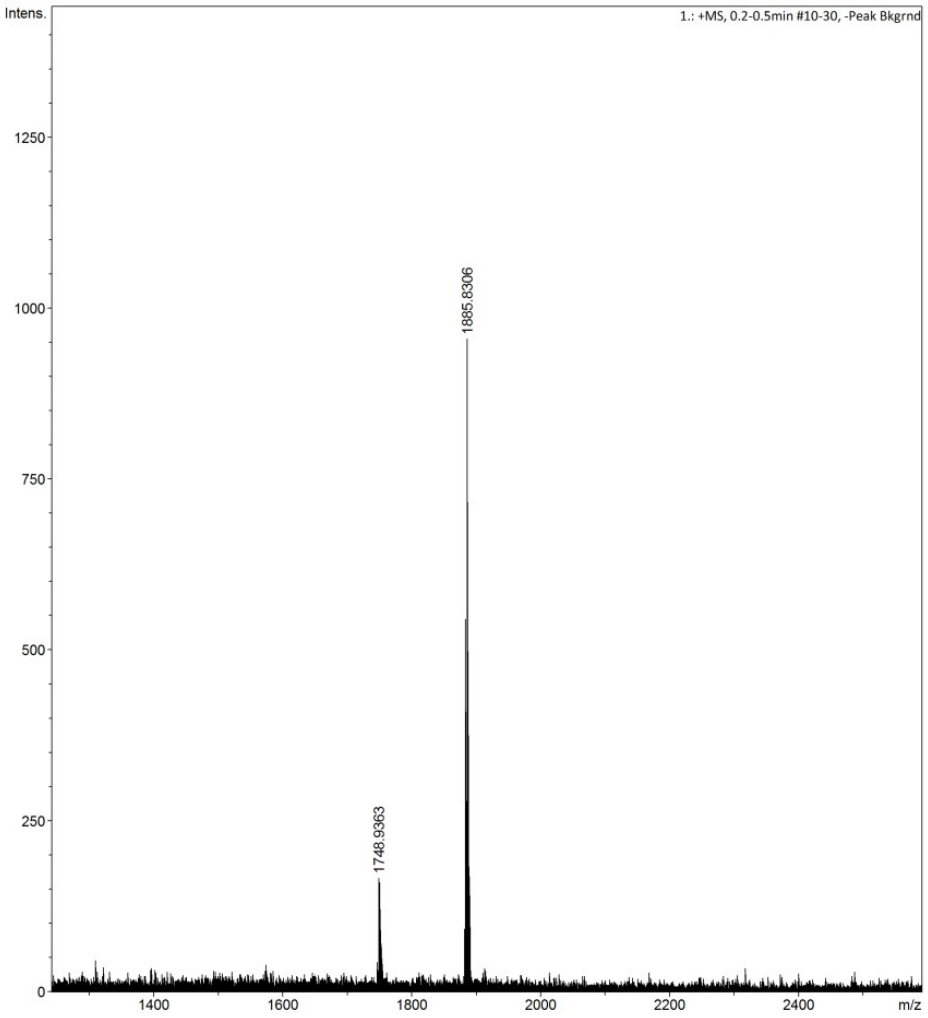

Fig. S10 The molecular ion peak of the intermediate in the catalytic oxidation process in MeCN/DMF solution

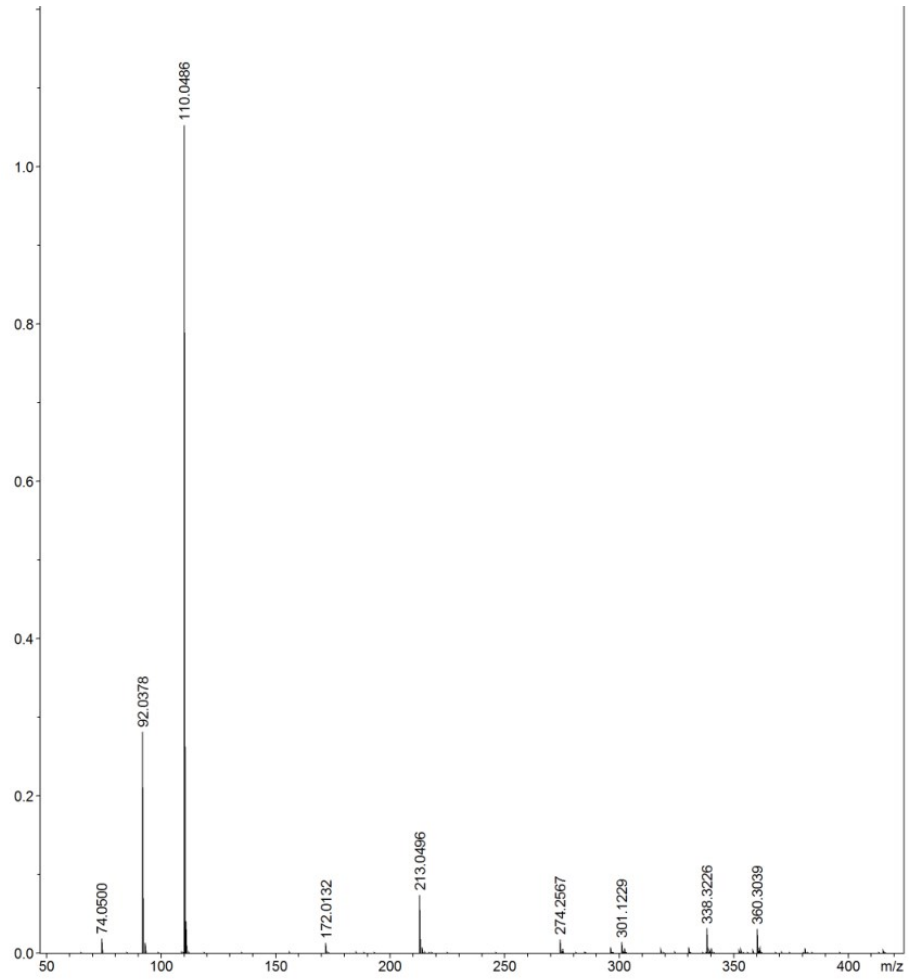

Figure. S11 Representative ESI-MS of APX.

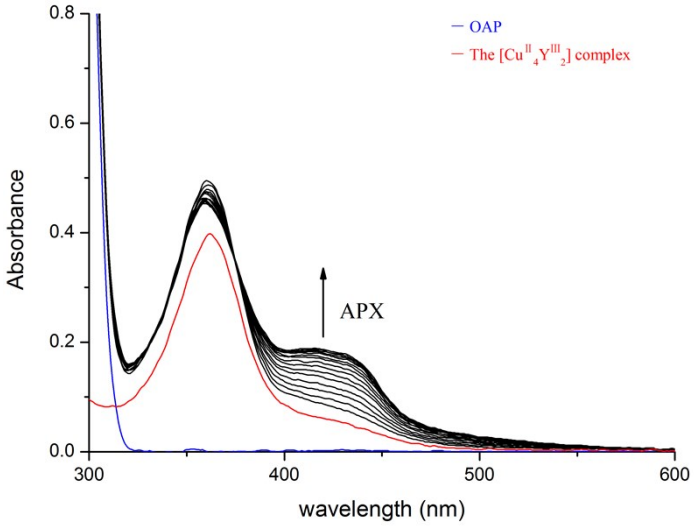

Fig. S12 Changes observed in UV-vis spectra of the $[Cu^{II}_4Y^{III}_2]$ complex in CH_3OH/DMF solution upon addition of 300-fold 2-aminophenol.

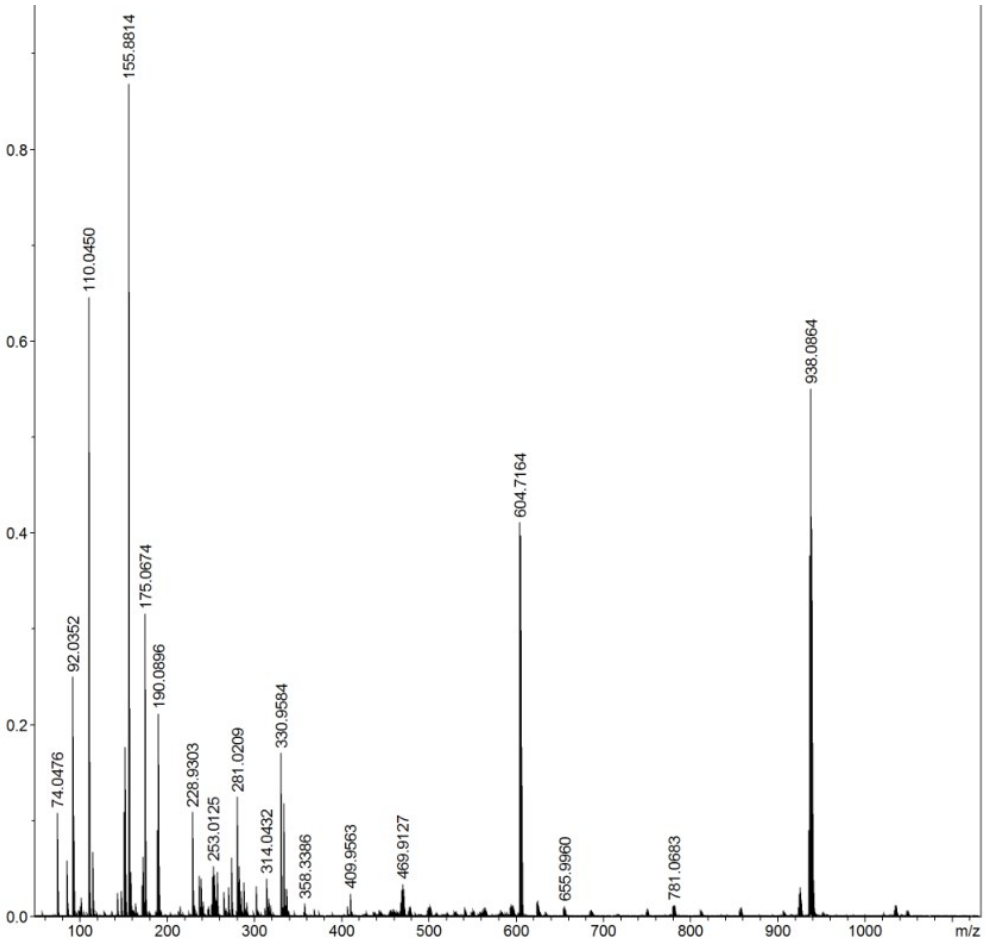

Fig. S13 Molecular ion peak of the intermediate in the catalytic oxidation process.

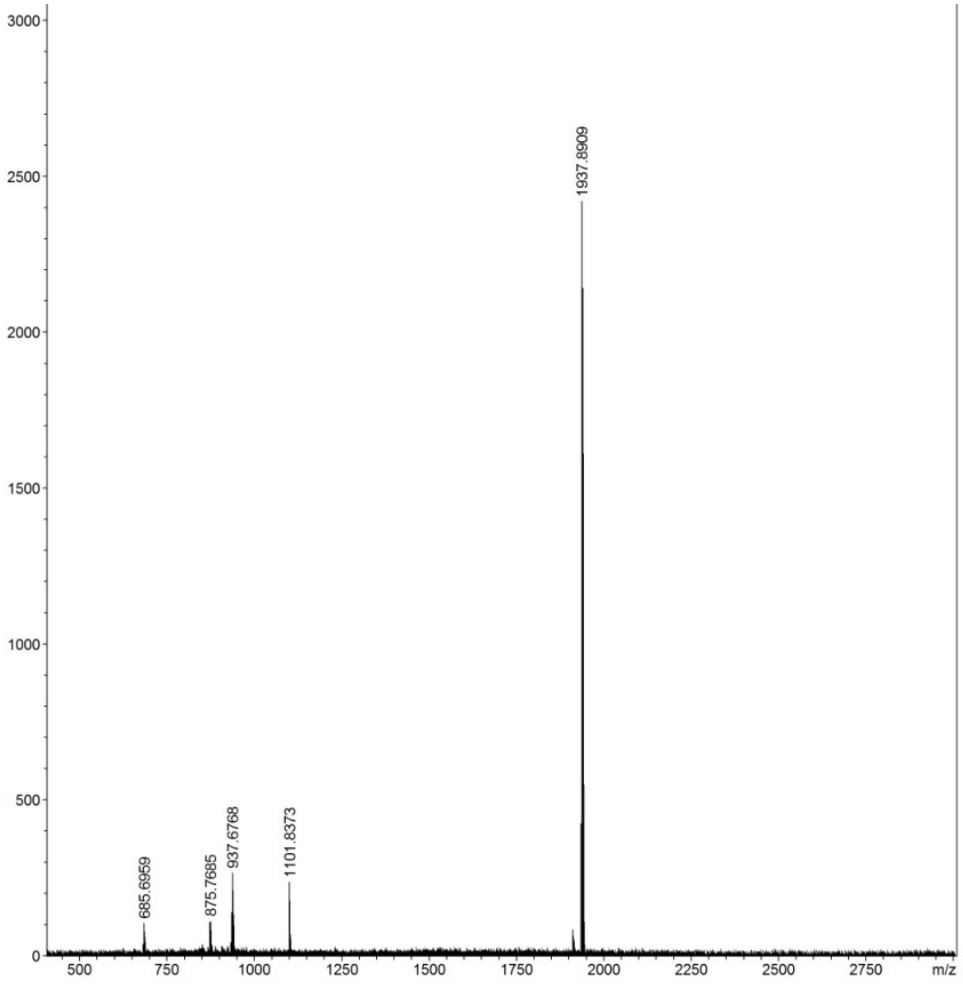

Fig. S14 The molecular ion peak of the intermediate in the catalytic oxidation process

Table S1 Main bond lengths and angles of the [$Cu^{II}_2Ce^{III}$] and [$Cu^{II}_4Y^{III}_2$] complexes.

The [$Cu^{II}_2Ce^{III}$] complex					
Bond	Lengths	Bond	Lengths	Bond	Lengths
Ce1-O1	2.563(3)	Ce1-O6	2.461(3)	Ce1-O7	2.459(3)
Ce1-O8	2.593(3)	Ce1-O9	2.573(3)	Ce1-O11	2.711(3)
Ce1-O12	2.558(3)	Ce1 -O13	2.597(4)	Ce1-O15	2.679(3)
Ce1-O16	2.559(3)	Cu1-O7	1.905(3)	Cu1-O8	1.943(3
Cu1-N3	2.009(4)	Cu1-N4	1.897(4)	Cu2-O1	1.959(3)
Cu2-O6	1.921(3)	Cu2-N1	1.925(3)	Cu2-N2	2.015(3)
Bond	Angles	Bond	Angles	Bond	Angles
O1-Ce1-O6	62.59(9)	O8-Ce1-O15	114.25(9)	O6-Ce1-O8	115.93(9)
O1-Ce1-O7	117.66(9)	O8-Ce1-O16	68.08(10)	O6-Ce1-O9	77.43(10)
O1-Ce1-O8	178.35(9)	O9 -Ce1-O11	48.27(9)	O6-Ce1-O11	111.33(9)
O1-Ce1-O9	69.94(9)	O9-Ce1-O12	124.52(10)	O6-Ce1 -O12	133.00(10)
O1-Ce1-O11	115.65(9)	O9-Ce1-O13	85.65(11)	O6-Ce1-O13	158.31(11)
O1-Ce1-O12	85.16(9)	O9 -Ce1-O15	131.09(9)	O6-Ce1-O15	66.46(9)
O1-Ce1-O13	99.00(12)	O9-Ce1-O16	146.87(10)	O6-Ce1-O16	74.32(10)
O1-Ce1-O15	64.66(9)	O11-Ce1-O12	113.30(10)	O11-Ce1-O16	130.11(9)
O1-Ce1-O16	110.53(9)	O11-Ce1-O13	64.55(11)	O12-Ce1-O13	49.37(12)
O6-Ce1-O7	61.88(9)	O11-Ce1-O15	177.50(9)	O12 -Ce1-O15	69.14(10)
O12 -Ce1-O16	87.84(10)	O7-Ce1 -O8	61.42(9)	O7-Ce1 -O13	125.61(12)
O13-Ce1 -O15	117.94(11)	O7-Ce1-O9	72.54(10)	O7-Ce1 -O15	113.77(9)
O13-Ce1-O16	125.51(11)	O7-Ce1-O11	63.79(10)	O7-Ce1-O16	79.04(10)
O15-Ce1-O16	48.65(9)	O7-Ce1-O12	156.48(10)	O8-Ce1-O9	110.67(9)
O8-Ce1-O11	65.37(9)	O8-Ce1-O13	82.61(12)	O8-Ce1-O12	95.63(9)
The [$Cu^{II}_4Y^{III}_2$] complex.					

Bond	Lengths	Bond	Lengths	Bond	Lengths
Y1-O1	2.424(4)	Y1-O8	2.394(4)	Y1-O12	2.411(4)
Y1-O4	2.348(4)	Y1-O9	2.405(4)	Y1-O13	2.619(4)
Y1-O5	2.365(4)	Y1-O10	2.451(4)	Y1-O16	2.294(4)
Y2-O17	2.386(4)	Y2-O20	2.377(4)	Y2-O21	2.314(4)
Y2-O24	2.377(4)	Y2-O25	2.431(4)	Y2-O26	2.440(4)
Y2-O28	2.354(4)	Y2-O31	2.517(4)	Y2-O32	2.448(4)
Bond	Angles	Bond	Angles	Bond	Angles
O1-Y1-O4	63.59(14)	O8-Y1-O16	87.00(14)	O4-Y1-O10	128.12(14)
O1-Y1-O5	125.29(13)	O8-Y1-N7	87.39(13)	O4-Y1-O12	91.01(13)
O1-Y1-O8	162.37(13)	O9-Y1-O10	52.71(13)	O4-Y1-O13	68.56(13)
O1-Y1-O9	88.40(14)	O9-Y1-O12	119.01(13)	O4-Y1-O16	84.47(14)
O1-Y1-O10	76.15(14)	O9-Y -O13	118.74(13)	O4-Y1-N7	143.39(14)
O1-Y1-O12	118.33(14)	O9-Y1-O16	73.99(13)	O5-Y1-O8	64.63(14)
O1-Y1-O13	67.92(13)	O9-Y1-N7	26.43(13)	O5-Y1 -O9	130.77(14)
O1-Y1-O16	82.09(14)	O10-Y1-O12	80.14(13)	O5-Y1-O10	155.49(14)
O1-Y1-N7	80.47(12)	O10-Y1-O13	66.71(12)	O5-Y1-O12	78.72(14)
O4-Y1-O5	64.67(14)	O10-Y1-O16	122.11(14)	O5-Y1-O13	107.74(13)
O4-Y1 -O8	129.19(14)	O10-Y1-N7	26.32(12)	O12-Y1-O16	154.34(14)
O4-Y1 -O9	146.93(14)	O12-Y1 -O13	50.41(14)	O12-Y1-N7	100.68(12)
O13-Y1-O16	146.11(14)	O13-Y1-O16	146.11(14)	O17-Y2-O21	126.75(14)
O13-Y1-N7	92.53(12)	O13-Y1-N7	92.53(12)	O17-Y2-O24	163.48(14)
O16-Y1-N7	97.87(13)	O16-Y1-N7	97.87(13)	O17-Y2-O25	95.34(14)
O17-Y2-O20	63.70(14)	O17-Y2-O20	63.70(14)	O17-Y2-O26	74.78(14)
O5-Y1-O16	76.52(14)	O17-Y2-O28	93.17(13)	O20-Y2-O26	123.56(13)
O5-Y1-N7	151.52(13)	O17-Y2-O31	122.72(13)	O20 -Y2 -O28	73.57(14)
O8-Y1-O9	75.25(14)	O17-Y2-O32	76.37(13)	O20-Y2-O31	114.36(14)

O8-Y1-O10	98.35(14)	O20-Y2-O21	64.71(14)	O20-Y2 -O32	75.24(14)
O8-Y1-O12	76.34(14)	O20-Y2-O24	123.76(14)	O21-Y2-O24	65.88(14)
O8-Y1-O13	125.78(13)	O20-Y2-O25	157.28(13)	O21 -Y2-O25	132.02(13)
O21-Y2-O32	78.86(14)	O24-Y2-O32	118.94(13)	O21-Y2 -O26	149.80(14)
O24-Y2-O25	78.81(14)	O25-Y2-O26	52.26(13)	O21-Y2-O31	69.54(14)
O24-Y2-O26	89.63(14)	O25-Y2-O28	118.74(14)	O26-Y2 -O28	72.37(14)
O24-Y2-O28	76.61(13)	O25-Y2-O31	68.29(14)	O26-Y -O31	119.92(13)
O24-Y2-O31	69.72(13)	O25-Y2-O32	92.00(14)	O26-Y2-O32	130.44(14)
O28-Y2-O31	143.53(13)	O28-Y2-O32	148.55(14)	O31-Y2-O32	51.38(13)

Table S2 The hydrogen bonding interactions (Å,°) of the [$Cu^{II}_2Ce^{III}$] and [$Cu^{II}_4Y^{III}_2$] complexes.

D–H···A	d(D–H)	d(H···A)	d(D···A)	∠D–H···A
The [$Cu^{II}_2Ce^{III}$] Complex				
D-H···A	D-H	H···A	D···A	D-H···A
C11-H11···O13	0.95	2.58	3.501(6)	162
C13-H13A···O15	0.99	2.58	3.312(5)	131
C13-H13B···O12	0.99	2.45	3.093(5)	122
C29-H29···O16	0.95	2.37	3.225(5)	150
C34-H34···O12	0.95	2.43	3.346(5)	161
C37-H37B···O12	0.95	2.57	3.263(5)	158
The [$Cu^{II}_2Y^{III}$] Complex				
D-H···A	D-H	H···A	D···A	D-H···A
C10-H10···O9	0.95	2.47	3.035(6)	118
C27-H27B···O15	0.99	2.42	3.368(8)	161
C31-H31···O10	0.95	2.43	3.274(6)	147
C35-H35A···O10	0.94	2.52	3.168(5)	152
C50-H50···O25	0.95	2.43	3.252(8)	145
C52-H52B···O29	0.99	2.42	3.397(8)	167
C54-H54A··· O12	0.95	2.52	3.454(6)	168
C73-H73A···O26	0.95	2.54	3.269(8)	134
C73-H73A···O28	0.95	2.58	3.276(8)	130
O34-H34···O35	0.86	1.74	2.605(12)	174
O35-H35···O30	0.88	1.95	2.801(14)	164
O36-H36···O37	0.84	2.30	2.968(15)	136
O37-H37···O38	0.84	2.33	3.106(19)	154
O38-H38···O30	0.82	2.05	2.836 (17)	163
C3-H3A···O11	0.98	2.54	3.443(8)	153
C51-H51···O26	0.95	2.56	3.467	160

Table S3. Catecholase activity data for some Cu^{II} complexes .

Complex	Solvent used	k_{cat} (h^{-1})	References
$[Cu_3(L_4)(\mu\text{-}OAc)](ClO_4)_2$	CH3OH/H2O	80.28	1
$[Cu_3(\mu\text{-}OH)(dppi)_3(L5)_3]$	THF	16.2	2
$[Cu_3L](ClO_4)_2 \cdot 5H_2O$	C2H5OH/H2O	9.54	3
[Cu3(L)(CH3COO)3]. 3H2O	CH3OH	7.5	4
$[Cu_2(L)_2(benzoate)_2]$	CH3OH	943	5
$[Cu_2(L)_2]$	CH3OH	720	6
$[Cu_2(L)_2(2\text{-hydroxybenzoate})_2]$	CH3OH	698	7
[Cu(L)(Cl)](BF4)	CH3CN	480	8
$[Cu(L)I_2]$	DMF	63.72	9
$[Cu(H_2L)(ClO4)]$	CH3OH	58.68	10

References

1 R. E. H. M. B. Osório, A. Neves, T. P. Camargo, S. L. Mireski, A. J. Bortoluzzi, E. E. Castellano, W. Haase and Z. Tomkowicz, *Inorg. Chim. Acta*., 2015, **435**, 153–158.

2 S. Calancea, S. G. Reis, G. P. Guedes, R. A. A. Cassaro, F. Semaan, F. L.-Ortiz, M. G. F. Vaz, *Inorg. Chim. Acta*., 2016, **453**, 104–114.

3 A. Szorcsik, F. Matyuska, A. Bényei, N. V. Nagy, R. K. Szilágyie and T. Gajda, *Dalton Trans*., 2016, **45**, 14998–15012.

4 V. K. Bhardwaj, N. A.-Alcalde, M. Corbella and G, Hundal, *Inorg. Chim. Acta*., 2010, **363**, 97– 106. 40.

5 F. Sama, A. K. Dhara, M. N. Akhtar, Y.-C. Chen, M.-L. Tong, I. A. Ansari, M. Raizada, M. Ahmad, M. Shahid and Z. A. Siddiqi, *Dalton Trans*., 2017, **46**, 9801–9823.

6 S. Sarkar, A. Sim, S. Kim and H.-I. Lee, *J. Mol. Catal. A: Chem*., 2015, **410**, 149–159.

7 B. Kumari, S. Adhikari, J. S. Matalobos and D. Das, J. *Mol. Struct*., 2018, **1151**, 169–176.

8 S. Adhikari, S. Lohar, B. Kumari, A. Banerjee, R. Bandopadhyay, J. S. Matalobos and D. Das, *New J. Chem*., 2016, **40**, 10094–10099.

9 E. C. M. O-Wenker, M. A. Siegler, M. Lutz and E. Bouwman, *Dalton Trans*., 2015, **44**, 12196–12209.

10 Á. Kupán, J. Kaizer, G. Speier, M. Giorgi, M. Réglier, and F. Pollreisz, J. *Inorg. Biochem*., 2009, **103**, 389–395.